Research Article Adv. Mater. Lett. 2015, **6**(5), 442-445 Advanced Materials *Letters*

www.amlett.com, www.vbripress.com/aml, DOI: 10.5185/amlett.2015.5732 Published online by the VBRI press in 2015

Effect of heavy ion irradiation at low temperature in Fe-14Cr-0.2Ti-0.3Y_2O_3

Sruthi Mohan, S. Balaji, S. Amirthapandian*, C. David, B.K. Panigrahi

Material Physics Division, Indira Gandhi Centre for Atomic Research, Kalpakkam 603102, Tamil Nadu, India

*Corresponding author. Tel: (+91) 4427480081; E-mail: pandian@igcar.gov.in

Received: 13 October 2014, Revised: 20 December 2014 and Accepted: 28 December 2014

ABSTRACT

Fe-14Cr-0.2Ti-0.3Y_2O_3, ODS alloy samples are irradiated with 880 keV Fe^+ ions at 230 K and 300 K upto a damage of 40 dpa at the surface. Transmission electron microscopy studies reveal a reduction in sizes of oxide dispersions in the ion irradiated alloys as compared to the as-prepared specimens; with greater diminution for samples irradiated at 230 K. Although the ion irradiation conditions (stage III) are favorable for vacancies to couple with solute atoms to cause precipitate growth, it is shown that such effects are less pronounced here and the ballistic effects dominate to cause oxide particle dissolution. Copyright © 2015 VBRI Press.

Keywords: Oxide dispersion; strengthened steel; heavy ion irradiation; transmission electron microscopy.

Sruthi Mohan is working as a Scientific Officer in the Material Physics Division, Indira Gandhi Centre for Atomic Research, Kalpakkam. Her current research interests are radiation damage studies on nuclear structural materials.

S. Amirthapandian received his Ph.D. degree from University of Madras in 2004. Currently, he is working as a Scientific Officer at Indira Gandhi Centre for Atomic Research in India. From 2008 to 2010, he worked as a postdoctoral researcher at University of Stuttgart in Germany. His current research interests are radiation damage in nuclear materials and micro-structural study on materials. He is assistant professor at Homi Bhabha National Institute (HBNI), India.

B.K. Panigrahi received his Ph.D. from Indian Institute of Science, Bangalore, India. Currently he is heading both Accelerator Materials Science Section and Computational Materials Science Section in Indira Gandhi Centre for Atomic Research. His current research interests are radiation damage simulations, void swelling in reactor structural materials and ion irradiation effects on nanomaterials. He is a professor at Homi Bhabha National Institute (HBNI), India.

Introduction

Oxide dispersion strengthened (ODS) steels containing nanosized Y-Ti-O precipitates are promising candidates for core structural materials in nuclear applications **[1, 2]**. The thermally stable precipitates are responsible for resistance to void swelling and thermal creep at elevated temperatures; hence, there has been a growing interest to understand the various aspects of the oxide dispersions with respect to their density, size distribution and crystal structure. Significant progress has been made recently on the study of density, size distribution, crystal structure and interfacial structure of the oxide nanoparticles which are vital in trapping helium, thereby reducing radiation induced swelling. Therefore, the stability of precipitates under irradiation condition is imperative if the role played by the precipitates has to be sustained throughout the resident time of the material in a reactor.

The role of ion irradiation as a surrogate for neutron irradiation in studying micro-structural evolution, segregation, precipitate stability and for basic studies in radiation damage is well established **[3]**. Ion irradiation studies on ODS alloys have revealed that the irradiation conditions play a major role in the stability of precipitates. Robertson et al. **[4]** reported that irradiation with single Fe^+ ion and Dual (Fe^+ and He^+) ions result in particle stability up to 25 dpa/40 appm He at 873 K . A report on self ion irradiation at high temperature (500° C) in Fe-14Cr-1W-0.3Ti-0.6Y_2O_3 upto 150 dpa shows a slight decrease in number density with slight increase in oxide nano-particle size from 3 nm to 4.5 nm and it is attributed to the Ostwald ripening of the precipitates **[5]**. In ODS alloys (K1(Fe-19Cr-0.3W-0.3Ti-0.35Y_2O_3) and K4(Fe-19Cr-2W-4Al-

0.3Ti-0.35Y_2O_3)), the complex oxide particles (containing (Y, Ti) or (Y, Al)) are reported to be stable up to a dose of 150 dpa at 670 ºC**[6]** upon 6.4 MeV self ion irradiation. However, no data on particle size distribution before and after irradiation were given in ref. **[6]**. Certain et al. **[7]** reported that the dissolution of nanoparticles (average size 2.6 nm) after Ni ion irradiation of a 14YWT ODS steel at -75 ºC upto a dose of 100 dpa. However, stable particle population was seen at 600 ºC which suggests that radiation enhanced diffusion allowed ejected atoms to reform nanoparticles **[7].**

These results convey that irradiation temperature influences both growth and diminution of precipitates. Nelson et al. **[8]** have predicted the existence of a critical temperature below which dissolution rate exceeds growth rate and smaller particles grow by the dissolution of larger ones. Collision cascades can knock out solute atoms from precipitates by re-solution. If the temperature is high enough to allow diffusion, the ejected atom can either diffuse back into the precipitate, diffuse away or re-precipitate into a new particle.

In the present work, ion irradiation stability of oxide particles is studied at temperatures in the stage III (where vacancies are immobile) regime **[9]** where the flow of solute atoms back into the precipitate is inhibited. Our TEM results confirmed that ion irradiation induced oxide particle dissolution and the mechanism is discussed in the light of radiation enhanced diffusion and ballistic effects.

Experimental

Materials

In ODS alloy system, alloying with Cr stabilizes the bcc iron matrix and gives corrosion resistance. The Y and Ti form thermally stable oxygen rich nanoclusters in bcc Fe matrix that enhances the high temperature strength **[1]**. The composition of the alloy prepared for the present study is given in **Table 1.**

Table 1. The composition of the alloy chosen for present study (in *Wt%*).

Cr	Y_2O_3	Ti	C	Fe
14	0.3	0.2	0.02	Balance

Mechanical alloying is the preferred fabrication route compared to chemical methods and other metallurgical methods to obtain homogeneous dispersoid distributions in ODS alloys **[10]**. Ultra high pure powders of Fe, Cr, Ti and Y_2O_3 (< 99.99% from Alfa Aesor) are ball milled (Simolayer CM – 08) for four hours at 1000 rpm in argon atmosphere with ball to powder ratio 10:1. It was extruded at 1423 K and then subjected to quenching followed by tempering (heated to 1023 K for two hours and air cooled) to obtain the ODS alloy rod of 12 mm diameter with a well defined microstructure**[11]**.

Method

The ODS samples are irradiated with 880 keV Fe^+ ions using a 1.7 MV Tandetron accelerator. Specimens used for irradiation were in the form of 10 mm diameter disks which have been electro polished.

The ion irradiation was carried out at temperatures 230 K and 300 K. The SRIM **[12]** calculations show that the projected range of Fe^+ ions was around 2947 Å with a straggling of 969 Å. The displacement damage on the surface of the sample was 40 dpa at a dose rate of 7.4×10^{-4} dpa/sec.

To prepare TEM specimens, the ion irradiated 10 mm diameter disks were further thinned down to 50 microns and disks of 3 mm diameter were punched out. The irradiated surface was masked by applying lacomit and specimens were back thinned to perforation using electropolishing. The electrolyte (ethanol, 2-butoxy ethanol and perchloric acid in 7:2:1 ratio) was used for electropolishing and it was carried out at the temperature of ~ -35 °C. The samples were characterized with LIBRA 200FE (Carl Zeiss) high resolution transmission electron microscope (HRTEM) operated at 200 kV equipped with energy dispersive X-ray spectroscopy (EDS) analysis, scanning transmission electron microscopy (STEM) and in-column energy filter. The information limit of the microscope is 0.13 nm.

Results and discussion

Fig. 1(a) shows the bright field image of the as-prepared Fe–14Cr–0.2Ti–0.3Y_2O_3 alloys and it is evident that the oxide nanoparticles are present throughout the specimen. However, some nanoparticles appear bright and others dark due to their orientation with respect to the electron beam. From many low magnification images, the size of the oxide particles is measured and their size distribution estimated. The size distribution of the oxide particles in as-prepared Fe–14Cr–0.2Ti–0.3Y_2O_3 alloy is shown in **Fig. 2(a).**

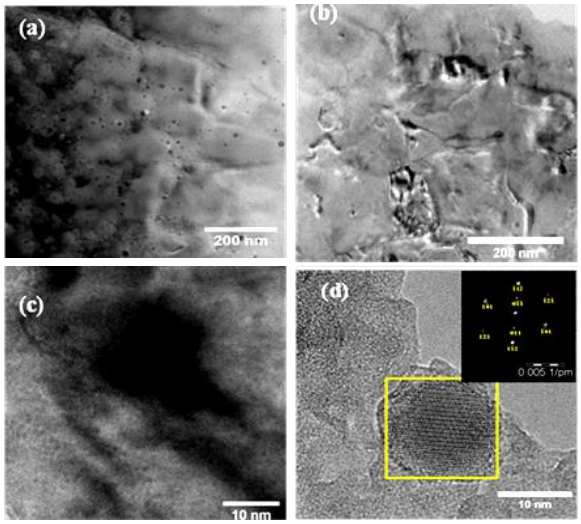

Fig. 1. The bright field image of the Fe–14Cr–0.2Ti–0.3Y_2O_3alloy sample (a) as-prepared, (b) 880 keV Fe^+ ion irradiated at 300 K and (c) at 230 K. The dose on the surface was 40 dpa in both the ion irradiated samples. The particles were very small (Fig. 1(c) in sample irradiated at 230 K. (d) The HRTEM image of the big oxide particle in Fe^+ ion irradiated specimen at 300 K. The inset shows the FFT from the highlighted region. From the *d* spacings ($d_{2\bar{1}1}$ =2.90 Å and d_{011}=3.51 Å) and the angle between the planes 53.9°.The crystal structure is Y_2TiO_5 and the zone axis is $3\bar{1}1$.

The size distribution is fitted with log-normal distribution. The oxide particle has sizes ranging from 1 to 35 nm, and most of particles are below 12 nm. The average size is found to be ~6.6 nm. The oxide particle density was estimated to be $7.9\times10^{20}/m^3$ and the number density is comparable with the reported values in the literature **[13].**

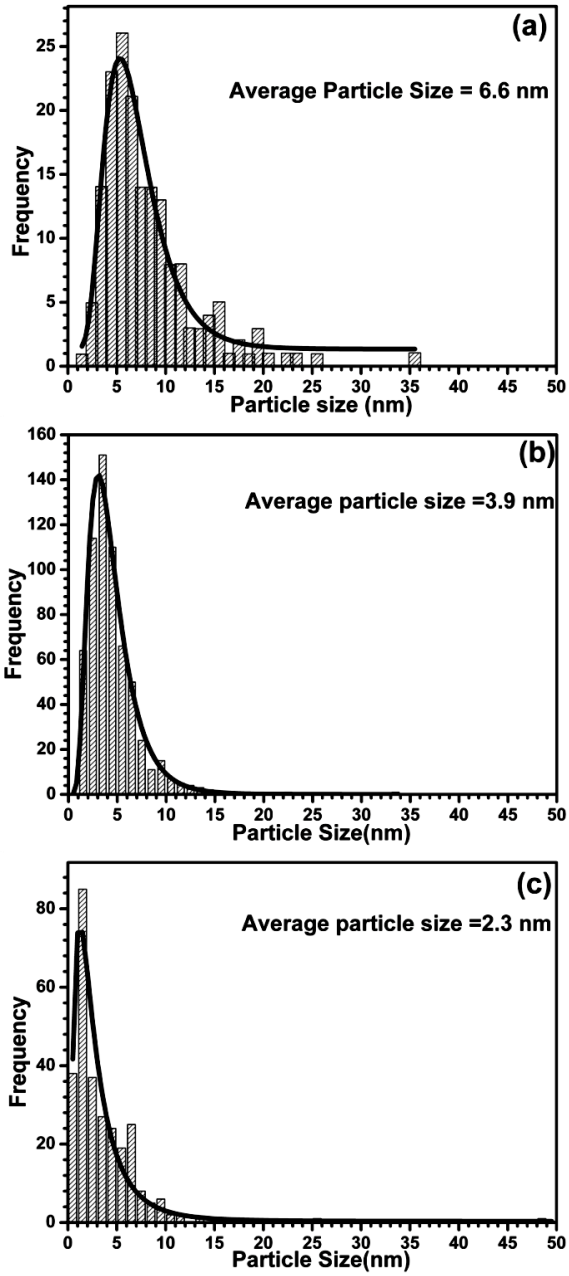

Fig. 2. The oxide particle size distribution of the Fe–14Cr–0.2Ti–0.3Y_2O_3 alloy sample (a) as-prepared, (b) 880 keV Fe^+ ion irradiated at 300 K and (c) at 230 K.The average particle size decreases upon ion irradiation.

The bright field image of the Fe–14Cr–0.2Ti–0.3Y_2O_3 alloy irradiated with Fe^+ ions at 300 K is shown in **Fig. 1(b)**. It clearly shows a reduction in particle size and particle density of oxide particles. The oxide particle size distribution was given in **Fig. 2(b)**. The average particle size and density is found to be 3.9 nm and $4.22\times10^{20}/m^3$ respectively. We did not observe any oxide particle greater than 20 nm in diameter and most of them were less than 10 nm in diameter. **Fig. 1(d)** shows the HRTEM image of the one of the bigger oxide particles in Fe^+ ion irradiated alloy at 300 K. The inset of Fig. 1(d) shows the fast Fourier transform (FFT) from the highlighted region. From the *d* spacing ($d_{1\bar{1}1}$ = 2.90 Å and d_{011}=3.51 Å) and the angle between the planes 53.9°, a confirmation that the crystal structure of the oxide particle is Y_2TiO_5 and the zone axis $3\bar{1}1$ is deduced.

Fig. 1(c) shows the bright field image of the Fe–14Cr–0.2Ti–0.3Y_2O_3 alloy irradiated with Fe^+ ions at 230 K. From many low magnification images, the sizes were measured and size distribution is given in **Fig. 2(c)**. It can be observed that the particles have not fully dissolved. The average particle size and particle density are estimated to be 2.3 nm and 2.3×10^{20} /m^3 respectively. **Fig. 3** shows the bright field image of the one of bigger particles (~100 nm) in the sample irradiated at 230 K. It can be observed that there is a halo of smaller particles around the big particle and this could well represent a case in which a displacement cascade is located within the big particle.

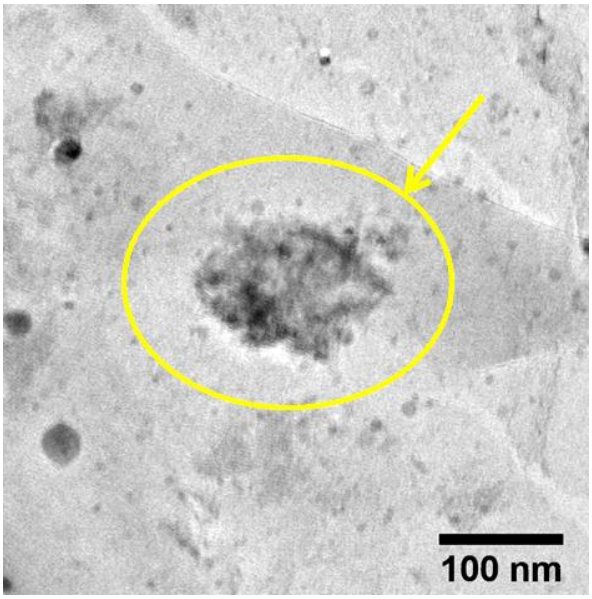

Fig. 3. The bright field image of the Fe–14Cr–0.2Ti–0.3Y_2O_3 alloy sample irradiated with Fe^+ ions at 230 K. In the highlighted region, a big oxide particle (~100 nm) is seen whose matrix-particle boundary has become irregular due to ion irradiation and very small particles are seen around the bigger particle.

In summary, the oxide particles in a ODS steel is not stable upon ion irradiation at 300 K and 230 K up to a dose of 40 dpa. The reduction in oxide particle size along with reduction in the particle density is observed in the present experiments. Our observation in larger particle upon ion irradiation (**Fig. 3**) is consistent with the literature **[13, 14]**. During heavy ion irradiation, the collision cascades can knock solute atoms out of oxide particles; and this is called re-solution. Once a solute atom has been ejected into the matrix, it can either diffuse back into the oxide particle, diffuse away into the matrix, or if the solubility limit in the matrix is reached, re-precipitate into a new oxide particle. In the present work, the ion irradiation has been carried out at sufficiently low temperatures (300 K and 230 K), where the ballistic diffusion is dominant over radiation enhanced diffusion.

The ballistic diffusion favours the production of homogeneous solid solution whereas radiation enhanced diffusion favours the accelerated diffusion towards equilibrium.

Table 2. Estimated values of characteristic time τ required for a vacancy to reach the sink.

Dose (dpa)	Irradiation Temp. (K)	Average Diameter (nm)	$k^2=4\pi R_p N_p$ ($/m^2$)	(m^2/sec)	τ (sec)
40	300	3.95	1.04×10^{13}	1.43×10^{-18}	3.35×10^{4}
40	230	2.3	3.32×10^{12}	3.78×10^{-22}	3.98×10^{8}

For a more quantitative approach, for irradiation at the temperature 230 K, the vacancy migration is expected to play a role because the temperature is in the range of stage(III) of resistivity recovery stage for bcc Fe after electron irradiation **[9]**. The characteristic time τ required for a vacancy to reach the sink with sink strength k is given by**[15]**,

$$t = \frac{1}{D_v k^2} \quad (1)$$

Here, D_v is the vacancy coefficient of diffusion. Here, nanoparticles act as sink for point defects and their sink strength is given by **[15]**

$$k^2 = 4\pi R_p N_p \quad (2)$$

where R_p is mean diameter of oxide particles and N_p is the oxide particle density. The R_p and N_p are measured from TEM experiments and given in **Table 2**. The vacancy diffusion coefficient is given as**[15]**,

$$D_v = \propto a^2 \vartheta \, exp\left(-\frac{E_v^m}{k_B T}\right) \quad (3)$$

where, E_v^m is the vacancy migration energy $(= 0.7eV)$, a is a geometric factor equal to 1, a is the lattice parameter for bcc iron $(= 0.287\ nm)$ and ϑ is the Debye frequency $(\vartheta = 10^{13}/\text{sec})$**[4]**. From **Table 2,** the characteristic time (τ) is found to be long, such that during ion irradiation, the annihilation at sinks is not possible. However, the characteristic time τ_p to reach recombination regime is $\tau_p=(1/RK_{IV})^{1/2}$, where K_{IV} is recombination rate of vacancies and interstitials and R is the ion flux. In the present experiments, $R = 7.4\times10^{-4}$ dpa/sec and $K_{IV} \sim 200\nu_I$ **[15]** where ν_I is jump frequency of interstitials.

Taking typical value of migration energy and jump frequency of interstitials, the calculated τ_p (=0.5s) clearly indicates that irradiation at room temperature is in the recombination regime, in which the concentration of vacancies is equal to that of interstitials. The concentration of vacancies due to irradiation $C_v^{irr} = (R/K_{IV})^{1/2} = 1.9\times10^{-4}$ for irradiation temperature of 300 K. The radiation enhanced diffusion co-efficient $D^{irr} = (C_v^{irr}/C_v^{eq})D^{th}$, and the calculated value of D^{irr} at room temperature irradiation is 2.3×10^{-22} cm^2/s. From TEM images, the average distance of recoil is measured to be 1 nm. Ballistic diffusion co-efficient calculated is $1.2 \times 10^{-18} cm^2/sec$. That means ballistic diffusion is $\sim10^4$ times higher than radiation enhanced diffusion. Since ballistic diffusion favors homogenization of solid solution, there will be dissolution of the chemical species of the oxide particle in bcc iron matrix.

Conclusion

Fe–14Cr–0.2Ti–0.3Y_2O_3, ODS alloy samples are irradiated with 880 keV Fe^+ ions at 230 K and 300 K upto a displacement damage of 40 dpa. Evaluation of the stability of oxide precipitates under ion irradiation was studied using Transmission electron microscopy and the study revealed that the particle sizes reduced during. Although these conditions are favorable for vacancies to couple with solute atoms to cause precipitate growth, it is shown for the first time that such effects are less pronounced and the ballistic effects dominate to cause oxide particle dissolution.

Acknowledgements
UGC, DAE and CSR are acknowledged for the TEM facility. R. Vijay from ARCI, Hyderabad is acknowledged for the help during alloy preparation.

Reference

1. Odette, G. R.; Alinger, M.J.; Wirth,B.D.; *Annu. Rev. Mater. Res.*, **2008,** *471-503*, 38. **DOI:**10.1146/annurev.matsci.38.060407.130315
2. Rebak, R. B.; *JOM*, **2014**, *2424*: 66. **DOI:** 10.1007/s11837-014-1211-9
3. Was, G. S.; Averback,R. S.; Radiation Damage Using Ion Beams, Comprehensive Nuclear Materials, Elsevier :Oxford, **2012**, p293. **DOI:** 10.1016/B978-0-08-056033-5.00007-0
4. Robertson, C.; Panigrahi, B.K.; Balaji S.; Kataria, S.; Serruys; Mathon, M.-H.; Sundar, C.S.; *J. Nucl. Mat.*, **2012**, *240-246*: 426. **DOI:** 10.1016/j.jnucmat.2012.04.001
5. Lescoat, M.-L.; Ribis, J.; Chen, Y., Marquis, E. A.; Bordas, E.; Trocellier, P.; Serruys, Y.; Gentils, A.; Kaitasov, O.; de Carlen, Y., Legris, A.; *Acta Materialia.*, **2014,** 328. **DOI:** 10.1016/j.actamat.2014.06.060
6. Kishimoto, H.; Yutani, K.; Kasada, R.; Hashitomi, O; Kimura, A.; J. *Nucl. Mat*, .**2007**, *179-184*, 367. **DOI:**10.1016/j.jnucmat.2007.03.149
7. Certain, A.; Kuchibhatla S.; Shutthanandan V.; Hoelzer D.T.; Allen, T.R.; *J. Nucl. Mat.*,**2013**, *311-321*, 434. **DOI:** 10.1016/j.jnucmat.2012.11.021
8. Nelson,R. S.; Hudson, J. A.; Mazey, D. J.; *J. Nucl. Mat.*, **1972**, *318-330*, 44. **DOI:** 10.1016/0022-3115(72)90043-8
9. Fu, C.C.; Torre, J.D.; Williame, F.; Bocquet, J.L.; Barbu, A.; *Nature Mater*. **2005,** *68-74*, 4. **DOI:** :10.1038/nmat1286
10. Gilman, P.S.; Benjamin, J. S.; *Ann. Rev. Mater. Sci.*, **1983**, *279-300*, 13. **DOI:** 10.1146/annurev.ms.13.080183.001431
11. Sundararajan, G.;Vijay, R.; Reddy, A.V.; *Current Science*, **2013,** *1100-1106*, 105.
12. Stopping Range of Ions in Matter **URL:** www.srim.org
13. Allen T.R.; Gan J.; Cole J.I.; Miller M.K.; Busby J.T.; Shutthanandan S.; Thevuthasan S.; J. *Nucl. Mat*, .**2008**, *26-37*, 375 **DOI:** 10.1016/j.jnucmat.2007.11.001
14. Monnet, I.; Dubuisson, V.; Serruys, Y.; Ruault, M. O.; Kaitasov, O; Jouffrey, B.; *J. Nucl. Mat.*, **2004**, *311-321*, 335. **DOI:** 10.1016/j.jnucmat.2012.01.026
15. Was, G. S.; Fundamentals of Radiation Materials Science Metals and Alloys; Springer, **2007.**